

Further developments in the local-orbital density-functional-theory tight-binding method

James P. Lewis,¹ Kurt R. Glaesemann,¹ Gregory A. Voth,¹ Jürgen Fritsch,² Alexander A. Demkov,³ José Ortega,⁴ and Otto F. Sankey⁵

¹Henry Eyring Center for Theoretical Chemistry and Department of Chemistry, University of Utah, 315 S. 1400 E., Rm. 2020, Salt Lake City, Utah 84112-0850

²Institut für Theoretische Physik, Universität Regensburg, D-93040 Regensburg, Germany

³Physical Sciences Research Labs, Motorola, Inc., Tempe, Arizona 85284

⁴Departamento de Física Teórica de la Materia Condensada, Universidad Autónoma de Madrid, E-28049 Madrid, Spain

⁵Department of Physics and Astronomy, Arizona State University, Tempe, Arizona 85217-1504

(Received 22 December 2000; revised manuscript received 27 March 2001; published 15 October 2001)

Improvements to the Sankey-Niklewaki method [O. F. Sankey and D. J. Niklewski, Phys. Rev. B **40**, 3979 (1989)] for computing total energies and forces, within an *ab initio* tight-binding formalism, are presented here. In particular, the improved method (called FIREBALL) uses the separable pseudopotential (Hamann or Troullier) and goes beyond the minimal sp^2 basis set of the Sankey-Niklewski method, allowing for double numerical basis sets with the addition of polarization orbitals and d orbitals to the basis set. A major improvement includes the use of more complex exchange-correlation functionals, such as Becke exchange with the Lee-Yang-Parr correlation. Results for Cu and GaN band structures using d orbitals within the improved method are reported; the results for GaN are greatly improved compared to the minimal basis results. Finally, to demonstrate the flexibility of the method, results for the H₂O dimer system and the energetics of a gas-phase octahydro-1,3,5,7-tetranitro-1,3,5,7-tetrazocine molecule are reported.

DOI: 10.1103/PhysRevB.64.195103

PACS number(s): 71.15.Ap, 31.10.+z

I. INTRODUCTION

Quantum-mechanical methods have become increasingly reliable as a complementary tool to experimental research. A variety of methods exist ranging in complexity from semi-empirical methods to density-functional-theory (DFT) methods [using either the local-density approximation (LDA) or the generalized-gradient approximation (GGA)] to methods for highly correlated systems (such as multiconfiguration self-consistent field or coupled clusters). Depending on the approximation used, such methods have been effectively applied to a variety of materials and systems.

With the increase in computational power, greater efforts have been made by the electronic-structure community to optimize the performance of quantum-mechanical methods. Calculating larger systems without making stringent approximations has only been possible within the past few years. Previously, usually only calculations with a minimal basis set, nontransition metals, or model systems, which consider no influence from the environment (in order to reduce the size of the problem), could be considered within these calculations. Now with advances in computational power and algorithms, calculations that use double- z (or double numerical) basis sets, plus polarization orbitals, are becoming the norm; also an increasing number of electronic-structure methods now incorporate d orbitals, which are needed in the simulation of transition metals and related compounds, therefore more complex systems are being studied with quantum-mechanical methods.

Within a tight-binding-like formalism more complex problems can be investigated with a modest decrease in the accuracy. This is particularly useful where a quantum-mechanical description is important to the investigated system's fundamental chemistry, but where a smaller model sys-

tem would inadequately describe the proper physical environment. In addition, there are even larger systems (i.e., enzymes or zeolites), which can only be currently calculated using these approximate methods; using more exact methods would be computationally unattainable.

One of the first reported approaches using an *ab initio* tight-binding formalism was the development of the Sankey-Niklewski SN method.¹ This method is based on norm-conserving pseudopotentials^{2,3} and the local-density approximation LDA limit of DFT, but uses the Harris-Foulkes functional^{4,5} and a minimal nonorthogonal local-orbital basis of slightly excited orbitals.^{1,6} The electronic eigenstates are expanded as a linear combination of pseudoatomic orbitals within a localized sp^3 basis for the atoms. These localized pseudoatomic orbitals, which we refer to as “fireballs,” are slightly excited due to the boundary condition that they vanish at some radius r_c [$\psi_{\text{fireball}}^{\text{atomic}}(r)|_{r \geq r_c} = 0$] instead of the “atomic” boundary condition that they vanish at infinity. The SN method and the improved method presented here include periodic boundary conditions.

Several studies on a variety of systems have shown the SN method to be an efficient and successful tool for performing electronic-structure calculations (for example, see Refs. 6–10). Other similar methods that evolved from the SN method have been successfully applied to a variety of systems.^{11,12} A self-consistent extension to the SN method has been developed and implemented because the non-selfconsistent nature of the Harris-Foulkes functional limits its applications to systems without a significant difference in the electronegativity of the system's constituents. This self-consistent procedure introduces a new degree of flexibility, adding the possibility of optimizing the input electron density ρ_{in} according to the chemical environment of the atoms.

The self-consistent method was originally developed and successfully applied to complex silicas,¹³ and recently results have been obtained for octahydro-1,3,5,7-tetranitro-1,3,5,7-tetrazocine (HMX).¹⁴ This method has also proved to be a very useful tool for dealing with complex-surface problems.^{15–19} In other work, hydrogen-bonded systems have been modeled by combining adequately the SN approach with a many-body method in which the exchange effects are described as a function of the orbital occupancies n_i .^{20,21} Implementation of a linear-scaling algorithm in addition to this hydrogen-bonding model provided for *ab initio* calculation of deoxyribonucleic acid (DNA).²²

Despite the several successful results referenced, the SN method is constrained by some underlying factors, such that the degree of complexity in the systems that could be investigated is limited. First, the form of the nonlocal pseudopotential is nonseparable;² therefore, more complex interactions involving three-center integrals must be computed (in a separable form of the nonlocal pseudopotential all the computed interactions can be reduced to two-center integrals²³). Second, one of the novelties of the SN method is that all interactions are precomputed exactly (up to three centers, no four centers are needed) and tabulated (the wave functions are zero beyond r_c); however, this is not the case for the exchange-correlation interactions. These interactions were not computed exactly, but rather approximated based on an average “effective” density. As a result, slight errors ($\sim 2\%$) in the exchange-correlation potential and energy occurred. Third, the LDA limit of DFT is the only functional available in the SN method. Fourth, in the past, inclusion of orbitals above a minimal basis set involved computationally intensive work, so the SN method avoided this extra complexity. Unfortunately, flexibility in the scope of the systems, which can be investigated in the original SN method, is limited.

In this paper, improvements to the SN method called FIREBALL are reported, which allow the performance of more accurate calculations in more complex systems. The feasibility of these improvements is now possible because of the continuing increase in computational power and because of better theoretical techniques. These improvements and results, which apply these improvements, are discussed in the paper as follows. Section II describes the theoretical basis of FIREBALL, discussing improvements made to the SN method. Results of FIREBALL are presented in Sec. III, with results for the Cu and GaN band structures in Sec. III B and III A, respectively. In addition, to demonstrate the flexibility of the method, results for the H₂O dimer are presented in Sec. III C. Finally, Sec. IV contains a summary and concluding remarks of FIREBALL in addition to further future developments.

II. THEORY

A. Theoretical foundation

The theoretical basis of the SN method is the use of the density-functional theory with a nonlocal pseudopotential scheme. At the core of the method is the replacement of the Kohn-Sham energy functional by the approximate Harris-Foulkes functional,^{4,5}

$$E_{\text{tot}}^{\text{Harris}} = E^{\text{BS}} + \{U^{\text{ion-ion}} - U^{\text{ee}}[\rho_{\text{in}}(\mathbf{r})]\} + \{U^{\text{xc}}[\rho_{\text{in}}(\mathbf{r})] - V^{\text{xc}}[\rho_{\text{in}}(\mathbf{r})]\}. \quad (1)$$

The main difference between the Kohn-Sham and Harris-Foulkes functional is that the latter is defined entirely in terms of an input charge density $\rho_{\text{in}}(\mathbf{r})$; whereas, the former is defined in terms of both an input and output charge density and the two converge when self-consistency is used. In Eq. (1) E^{BS} is the band-structure energy ($2\sum_{i \in \text{occ}} \epsilon_i$), where ϵ_i are the eigenvalues of the one-electron Schrödinger equation given by

$$\left\{ -\frac{\hbar^2}{2m} \nabla^2 + V_{\text{ext}}(\mathbf{r}) + \mu_{\text{xc}}[\rho_{\text{in}}(\mathbf{r})] + \frac{e^2}{2} \int \frac{\rho_{\text{in}}(r)}{|\mathbf{r}-\mathbf{r}'|} d^3 r' \right\} \psi_i(\mathbf{r}) = \epsilon_i \psi_i(\mathbf{r}). \quad (2)$$

The second term of Eq. (1) is the “short-range” repulsive interaction, which is the ion-ion interaction offset by the overcounting of the Hartree interactions. This term is given by

$$\{U^{\text{ion-ion}} - U^{\text{ee}}[\rho_{\text{in}}(\mathbf{r})]\} = \left\{ \frac{e^2}{2} \sum_{i,j} \frac{Z_i Z_j}{|\mathbf{R}_i - \mathbf{R}_j|} - \frac{e^2}{2} \int \frac{\rho_{\text{in}}(\mathbf{r}) \rho_{\text{in}}(\mathbf{r}')}{|\mathbf{r}-\mathbf{r}'|} d^3 r d^3 r' \right\}. \quad (3)$$

The last term of Eq. (1) is a correction to the exchange correlation, given by

$$\{U^{\text{xc}}[\rho_{\text{in}}(\mathbf{r})] - V^{\text{xc}}[\rho_{\text{in}}(\mathbf{r})]\} = \int \rho_{\text{in}}(\mathbf{r}) \{ \epsilon_{\text{xc}}[\rho_{\text{in}}(\mathbf{r})] - \mu_{\text{xc}}[\rho_{\text{in}}(\mathbf{r})] \} d^3 r. \quad (4)$$

This term arises because the one-electron Schrödinger eigenvalues contain the potential $\mu_{\text{xc}}[\rho_{\text{in}}(\mathbf{r})]$; however, the correct exchange-correlation interaction energy is the integral $\int \rho_{\text{in}}(\mathbf{r}) \epsilon_{\text{xc}}[\rho_{\text{in}}(\mathbf{r})] d^3 r$. In general, the construction of formulas for the hopping-matrix elements is outlined in the original SN paper. With the given form of the total energy, the forces acting on an atom at position R_l are determined by taking the derivative of the total energy with respect to R_l . The band-structure force is evaluated using a variation of the Hellmann-Feynman theorem.¹

In solving the one-electron Schrödinger equation of Eq. (2), a set of slightly excited pseudoatomic “fireball” wave functions are used. These orbitals are computed within DFT and a norm-conserving separable pseudopotential²³ and are chosen such that they vanish at some radius $r_c(\psi_{\text{fireball}}^{\text{atomic}}|_{r \geq r_c} = 0)$. This boundary condition is equivalent to an “atom in the box” and has the effect of raising the electronic energy levels ($\epsilon_a, \epsilon_p, \epsilon_d, \dots$ atomic eigenvalues) due to confinement. The radial cutoffs r_c are chosen such that these electronic eigenvalues remain negative and are mildly perturbed from

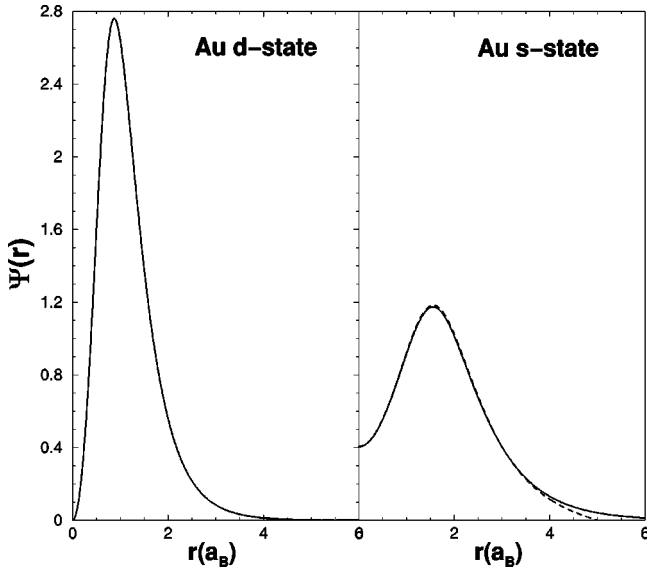


FIG. 1. The slightly excited pseudoatomic orbitals for the d state and s state of Au (solid line, free-atomic wave function; dashed line; “fireball” wave functions).

the free atom. This methodology is also used in the SIESTA technique¹¹ and the given excitation energies are used to determine r_c 's.

Figure 1 shows a comparison between the “fireball” wave functions and the free-atomic wave functions (s , p , and d for Au). It is very important that the r_c 's are chosen to preserve the chemical trends of the atoms, i.e., the excitation of the atoms must be done in a manner that preserves the relative ionization energies and relative atomic sizes. A theoretical basis for judiciously choosing these r_c 's was discussed in a previous work.⁶ For this example, an excitation energy of ~ 2.0 eV was chosen to determine the cutoffs, yielding $r_c^{5d} = 4.7a_B$ and $r_c^{6a} = 5.0a_B$. Note that for the Au d state there is no distinguishable difference in the exact wave function and the wave function with $r_c^{5d} = 4.7a_B$.

The “fireball” boundary condition yields two promising features. First, the range of hopping-matrix elements between orbitals on different atoms is limited; therefore, very sparse matrices are created for large systems. This inherent sparseness allows one to more readily implement linear-scaling algorithms to obtain the band-structure energy. Second, the slight excitation of the atoms somewhat accounts for Fermi compression in solids, which apparently gives a better representation of solid-state charge densities.²⁴ In the SN method, only a minimal sp^3 basis set was implemented, which limited the flexibility of the method. The improved method presented here (called FIREBALL) now allows a more flexible choice of basis set where double-numerical (DN) or additional-polarization sets are permitted. Earlier work shows that the addition of the DN set yields very good results in *ab initio* tight-binding methods that are similar to FIREBALL.^{11,12}

In evaluating the total energy of the system [Eq. (1)], the input density is a sum of confined spherical atomic-like densities,

$$\rho_{in}(\mathbf{r}) = \sum_i n_i |\phi_i(\mathbf{r} - \mathbf{R}_i)|^2. \quad (5)$$

The orbitals $\phi_i(\mathbf{r} - \mathbf{R}_i)$ are the slightly excited “fireball” pseudoatomic wave functions, which are used as basis functions for solving the one-electron Schrödinger equation [Eq. (2)]. The occupation numbers n_i determine the number of electrons occupying each spherically confined atomic-like density. In the Harris-Foulkes approximation implemented within the SN method, the input density is not determined self-consistently, but rather the occupations numbers are taken from a reference “atomic” density ($n_i = n_i^0$). It has been shown that the Harris total energy functional has errors that are only second order in the errors of the input density.^{1,4}

B. Pseudopotential approximation

In the SN method the form of the nonlocal pseudopotential is nonseparable,² therefore, more complex interactions involving three-center integrals must be computed. To simplify this, the separable form of the nonlocal pseudopotential is used so that all the computed interactions can be reduced to two-center integrals.²³

The pseudopotentials (also known as effective core potentials) are derived from the solution of the Schrödinger equations for the all-electron eigenstates of the free atom. Relativistic and other core-region effects are included by incorporating averaged spin-orbit coupling, the mass-velocity and Darwin terms, and the effective all-electron potential given as the sum of the Hartree potential, the exchange-correlation potential, and the electrostatic potential of the nucleus. For the exchange-correlation energy and, respectively, for the exchange-correlation potential, various parametrizations of the LDA and of the GGA are available.^{25–32}

The pseudopotential and pseudoatomic wave functions may be generated in the Hamann form or in the Troullier-Martins form as discussed in detail in Refs. 23 and 33, employing the scheme of Fuchs and Scheffer.³⁴ For the representation of the pseudopotentials in their semilocal form, the local potential is calculated for $l_{loc} = l_{max} + 1$ and $\epsilon_{l_{loc}} = \epsilon_{l_{max}}$, where l_{max} is the momentum of the highest occupied orbital and $\epsilon_{l_{max}}$ is its energy. With the choice of $l_{loc} = l_{max} + 1$ for the local part, unphysical “ghost” states are usually avoided when the pseudopotential is transformed into the fully separable form of Kleinman and Bylander.³⁵ The absence of ghost states is checked by examining the band-state spectrum using the analysis of Gonze Stumpf, and Scheffler.³⁶

C. Exchange-correlation interactions

In the SN method, the exchange-correlation interactions were not computed exactly, but rather approximated based on the “nearly uniform-density approximation.” A better approach for calculating the exchange-correlation (XC) interactions was proposed by Horsfield,¹² which uses a many-center expansion based on an expansion of the density, a site at a time. This method provides advantages over the approximations, which were utilized in the SN method. Primarily,

this is a higher-order approximation than the nearly uniform-density approximation and it can be used with gradient-corrected functionals. The XC potential matrix elements are calculated by including up to three centers in the approximation; however, the on-site terms use only up to a two-center approximation. The exchange-correlation double-counting correction is also calculated using a two-center approximation.

This approach for calculating exchange-correlation interactions as presented in Eqs. (6)–(8) of Ref. 12 facilitates storing integrals in tables in the same manner as the electrostatic integrals, the two-center approximation for the exchange-correlation contribution to the crystal-field results in this contribution always being overestimated. On occasion this may result in poor geometries or ghost states. In this situation, a correction must be added to the two-center approximation as explained in Ref. 12.

This approach for determining the exchange-correlation interactions is independent of the type of functional used. Currently two types of exchange-correlation density functionals are available within FIREBALL-LDA and Becke exchange (Ref. 28) with Lee-Yang-Parr (LYP) correlation.²⁷ Within the LDA, the exchange-correlation energy is designed to exactly reproduce the energy and potential of the uniform electron gas^{37,25} ($dn/dr=0$); however this approach underestimates the exchange energy, because exchange increases with increased density variability. Conversely, LDA consistently overestimates correlation energy. To improve upon the chemistry predicted by the LDA approach, functionals that depend upon the gradient of the density were developed.

For exchange interactions, the Becke-exchange functional ($E^{\text{exchange}} \equiv E[n(\mathbf{r}), \nabla n(\mathbf{r})]$) has enjoyed popularity,²⁸ particularly because it has only one empirical parameter that is fit to the exchange energies of the noble gases. The presence of a single parameter was an improvement over earlier multiparameter functionals.³⁸ Similarly, the LYP gradient-corrected correlation functional ($E^{\text{correlation}} \equiv E[n(\mathbf{r}), \nabla n(\mathbf{r})]$) has also enjoyed popularity.²⁷ It is a reformulation of the correlation formulas of Colle and Salvetti³⁹ in terms of the electron density and the local kinetic-energy density. The combination of Becke and LYP (BLYP) has proven to provide reliable energetics and molecular geometries.⁴⁰ As of this work, BLYP is the most favored DFT exchange-correlation functional, largely as a result of its effectiveness in predicting molecular properties and its presence in popular quantum-chemistry codes.

D. Self-consistency implementation

The Harris-Foulkes approximation is shown to work quite well for a variety of systems, especially those that are strongly covalent.⁶ Tests on this functional have shown that it yields total energies, which are remarkably similar to the LDA approximation but lie below them rather than above them as in a variational Kohn-Sham calculation. Several studies of this functional exists in the literature,^{41–46} and the reader is directed to these references for details. However, due to the non-self-consistent nature of the Harris functional, its applications are limited to systems without a significant difference in the electronegativity of their constituents.

The FIREBALL method has been generalized to deal with systems that exhibit a significant transfer of charge between atoms and require a self-consistent determination of the occupation numbers n_i , i.e., now $n_i = n_i^0 + \delta n_i$. Thus, the total energy is a *function* of the occupation numbers, $E_{\text{tot}}[\rho_{\text{in}}(\mathbf{r})] \equiv E_{\text{tot}}[n_i](n_i \neq n_i^0)$, and a self-consistent procedure on the occupation numbers n_i is introduced. A more detailed description of this self-consistent method used (referred to as DOGS) is found in Refs. 6 and 13.

When self-consistency is considered, the exchange-correlation interactions must take into account the change in the charge distributions between atoms. The procedure for evaluating the Hamiltonian matrix elements and the double-counting term for the exchange-correlation interactions is outlined in Ref. 12. The underlying idea is that because the exchange-correlation interactions vary with the change in the occupation numbers, δn_i , these interactions can be approximated by an expansion about $\delta n_i = 0$. A linear expansion is used for the terms in the Hamiltonian and a quadratic approximation is used for the double-counting term.

E. Localized orbitals and basis sets

The use of localized “fireball” orbitals is found to be computationally advantageous. Given any two atomic orbitals i and j beyond some cutoff radius ($r_{ci} + r_{cj}$), the matrix elements H_{ij} and S_{ij} become exactly zero. Therefore, there is only a preprescribed interaction range over which the integrals must be evaluated. Within the FIREBALL approach integrals are precalculated on a numerical grid and the specific values needed are gleaned from the tabulated values via interpolation. Because these integral tables depend only on the atom type, their r_c values, and the type of DFT exchange-correlation functional used, the integral tables need to be generated only once, for a given number of atomic species, rather than once or more per molecular dynamics run. The “direct” approach⁴⁷ in which integrals are calculated as needed is similar to the approach taken within FIREBALL. This pregeneration process lends itself to parallelization via spreading of these integrals out over multiple processors based on integral types.^{48,49} This parallelization is particularly important, since the number of integrals needed grows as order N^3 with the number of different elements N .

The original SN method is limited to single-numerical basis sets of the minimal sp^2 type. Development of new basis sets and deciding what type of functions to use is currently an area of extensive research within the field of electronic structure. A common theme throughout this literature is that one often needs more than a minimal basis set. The basis-set limitations within the SN method made studying transition metals impossible given the lack of d orbitals and made it difficult to study chemical systems that required the additional flexibility that polarizing d functions and extra s and p shells might provide. The FIREBALL method now allows for d functions and as many orbitals as the user desires. The addition of d functions has been previously considered in a Sankey-Niiklewski approach, but with a different procedure for their implementation.¹⁰ There is nothing inherent to the method to formally disallow extensive f, g, h, \dots shells,

but the current implementation does not support them. This flexibility in generating the basis set allows the SN method to properly describe many chemical systems with only a single-numerical basis set.

DN basis sets are currently generated by holding the ground-state wave function fixed and exciting electron density to a higher orthogonal state with the same r_c value. There are other approximations for generating additional DN basis sets as discussed in Refs. 11, 12, and 50. Investigation of these other approaches within FIREBALL is the subject of future work. Polarizing d functions (unoccupied orbitals in the ground-state atom) are generated by exciting the electron density into a d shell with a well-chosen r_c value. It should be noted that the d shells used in FIREBALL consist of five spherical-harmonic d functions as opposed to the six Cartesian d functions used with some Gaussian basis sets. Polarization provides a flexibility in the basis set that was not available in the functions of lower angular momentum, and thus may improve the chemistry. Going beyond DN with polarization (DNP) is generally not necessary, because the DN basis set allows for a wide range of wave-function curvatures, and triple-numerical basis sets would not provide the same qualitative improvement over DN as DN did over single numerical.

III. RESULTS

A. GaN properties

Group-III nitrides attract much attention because of their potential in many technological applications. Important progress was achieved in the fabrication of electro-optical devices, leading to the realization of blue-light-emitting p - n junctions⁵¹ and laser diodes.⁵² The energy gap of GaN is 3.4 eV, lying between 1.9 and 6.2 eV measured for InN and AlN.⁵³ Hence, GaN is the key compound for group-III nitride alloys and heterostructures. GaN usually crystallizes in the wurtzite phase, which is the ground-state structure. Stabilization of the zinc-blende phase was reported for the growth of thin films on the (001) surfaces of GaAs, cubic SiC, MgO, and Si.⁵⁴ In electronic-structure calculations performed for GaN, it is essential to include explicitly semicore states in the computation.⁵⁵ This means that the $3d$ electrons of Ga have to be treated as valence states in the pseudopotential method in order to obtain correct bonding properties^{56,57} like the lattice parameter, bulk modulus, or relative energies of surface structures, defects and boundaries.

Here, the results obtained with FIREBALL for the zinc-blende phase of GaN are summarized. To study the effects introduced by including the semicore states of Ga, we compare the computed lattice parameter, bulk modulus, and electronic band structure determined with an sp^3 basis for Ga and N with the results obtained from an extended sp^3d^5 basis for Ga. The pseudopotentials of Ga and N were constructed in the Hamann scheme.²³ For the exchange-correlation functional, we employ the local-density approximation using the parametrization of Perdew and Zunger.²⁵ The “fireball” orbitals were constructed with a confinement radius of $3.90a_B$ for the $2s$ and $2p$ states of N, while the $4s$

TABLE I. Lattice constant a_0 , bulk modulus B_0 , and gap energy E_{gap} computed for zinc-blende GaN in the Harris-Foulkes approach and with the self-consistent charge-transfer approach (DOGS), using sp^3 - or sp^3d^5 -basis sets for Ga and a sp^3 -basis set for N. The values in parentheses summarize results obtained with (20%) smaller onsite two-center exchange-correlation matrix elements. Results from plane-wave local-density calculations (PW-LDA) (Ref. 57), Hartree-Fock calculations (HF) (Ref. 62), and from experimental results (Refs. 59–61) are included.

Basis	Charge transfer	a_0 (Å)	B_0 (Mbars)	E_{gap} (eV)
Ga(sp^3)	No	4.39	1.54	3.86
Ga(sp^3)	Yes	4.39	1.99	2.99
Ga(sp^3d^5)	No	4.33	2.58	3.09
Ga(sp^3d^5)	Yes	4.35	2.99	2.39
Ga(sp^3)	Yes	(4.52)	(1.64)	(2.58)
Ga(sp^3d^5)	Yes	(4.52)	(2.18)	(1.80)
PW-LDA		4.52	1.91	1.60
HF		4.52	2.54	
Experiment		4.52	1.90	3.45

and $4p$ orbitals of Ga are confined to a sphere with a radius of $5.40a_B$. For the Ga $3d$ states, $r_c=3.5a_B$ is used. Given this choice of cutoffs, the energies of both the N and Ga states are ~ 2 eV above the unperturbed levels of the free atoms.

Table I summarizes the lattice constant, bulk modulus, and gap energy calculated with the sp^3 - and sp^3d^5 -basis sets, using the Harris-Foulkes approach^{4,58,5} and using the self-consistent charge-transfer approach (DOGS) discussed in Sec. II D. Our results are compared with experimental data and previous theoretical work by others.^{57,59–62} The lattice constant is similar in all cases, while the bulk modulus is increased when charge transfer is taken into account. For both basis sets, the calculation underestimates the measured lattice constant by 3–4%. The bulk modulus is largely increased above the experimental value, when the Ga $3d$ states are included in the calculation. These deviations are partially related to the multicenter expansion of the exchange-correlation matrix elements, with the atom two-center contributions being always overestimated.¹² This can be easily checked by rescaling all respective two-center matrix elements by a constant factor $0 < \lambda < 1$. The lattice constant increases continuously with the degree of the reduction of the matrix elements. Good agreement with measured data for the lattice constant is achieved by this, the lattice constant is increased to 4.5 Å for both basis sets and self-consistent charge transfer. The bulk modulus is decreased to 2.18 and 1.64 Mbars for the sp^3d^5 - and sp^3 -basis sets, respectively. For a rigorous treatment, the multicenter expansion should be replaced by a direct evaluation of the exchange-correlation matrix elements in terms of numerical integration of many-center contributions. These contributions are not currently obtainable within the scope of interpolating two- and three-center integrals as done in the current method. However, implementing the proper correction to the exchange-correlation interactions, necessary in some cases, will be addressed in future work.

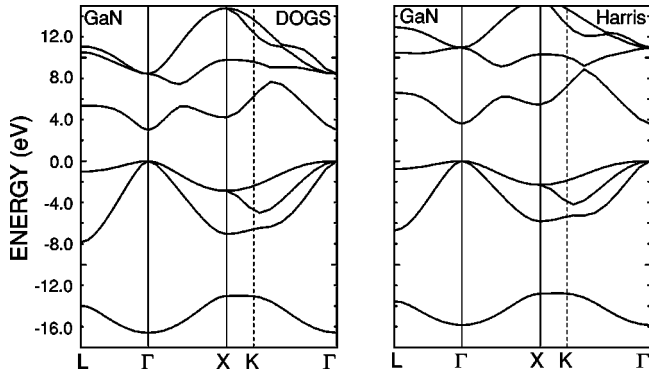


FIG. 2. Dispersion of zinc-blende-phase GaN computed with sp^3 -fireball orbitals for Ga and N. Left: self-consistent charge transfer included. Right: Harris-Foulkes approach.

Figures 2, 3, and 4 illustrate the electronic band structure of GaN computed with sp^3 - and sp^3d^5 -“fireball” orbitals, using the Harris-Foulkes approach and self-consistent charge transfer. In all cases, the corresponding theoretical lattice constant was used. The band structure correctly shows that zinc-blende-phase GaN has a direct band gap at the Γ point, with a separation of the valence and conduction bands as summarized in Table I. Charge transfer reduces the gap energies with respect to those of the Harris-Foulkes approach.

The electronic bands computed in the valence-band region and also the first conduction band agree nicely with the results of previous plane-wave calculations^{55,57} (noting that LDA typically gives band-gap values that are approximately 50% of experiment). Because of the small basis used in our approach, however, differences occur in the higher conduction bands. Consistent with the trends observed for the lattice constant, the agreement with previous computations is largely improved by reducing the atom two-center exchange-correlation matrix elements by 20%. Figure 4 shows that the gap energy is 1.8 eV in this case, which compares very well with the values from other pseudopotential methods as summarized in Ref. 57.

Effects of the transfer of electronic charge from the Ga atoms to the N atoms in GaN are clearly illustrated in Figs. 3 and 4. The Ga $3d$ bands are shifted downwards by about 3.5

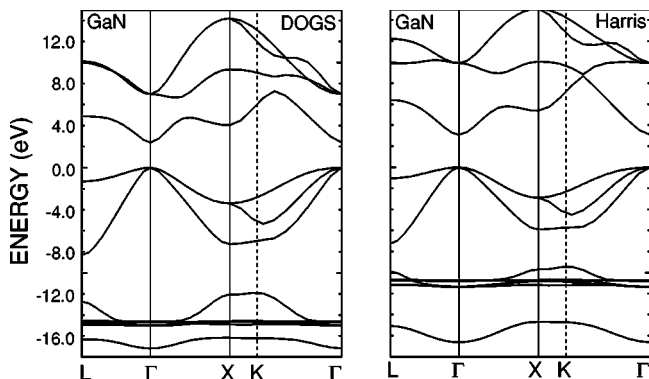


FIG. 3. Dispersion of zinc-blende-phase GaN computed with sp^3d^5 -fireball orbitals for Ga. Left: self-consistent charge-transfer included. Right: Harris-Foulkes approach.

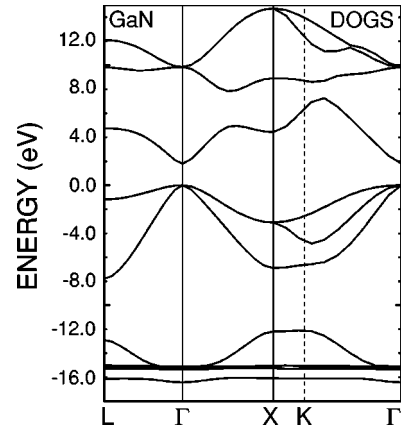


FIG. 4. Dispersion of zinc-blende-phase GaN computed with sp^3d^5 -fireball orbitals for Ga, including self-consistent charge transfer and a 20% reduction of the two-center atom contribution to the exchange-correlation-potential matrix elements.

eV, so that they finally lie in the energy region of the N $2s$ band in agreement with other density-functional calculations. The exact location of the $3d$ bands in GaN is found in experiments below the N $2s$ states.⁶³ This behavior is only reproduced by calculations that include self-interaction corrections,⁶⁴ but not by the usually applied LDA and GGA schemes.⁵⁵⁻⁵⁷ However, many properties of GaN, like the lattice parameter, bulk modulus, or relative energies of surface structures, defects and boundaries, are essentially not affected by the discrepancy in the relative location of the Ga $3d$ bands to the N $2s$ bands.

B. Cu band structure

In this section we use the band structure of Cu as an example to show the performance of FIREBALL for transition metals. Figure 5 shows the Cu band structure along several high-symmetry directions, as calculated using two different basis sets: (i) (dotted lines) a minimal sd^5 basis set of “fire-

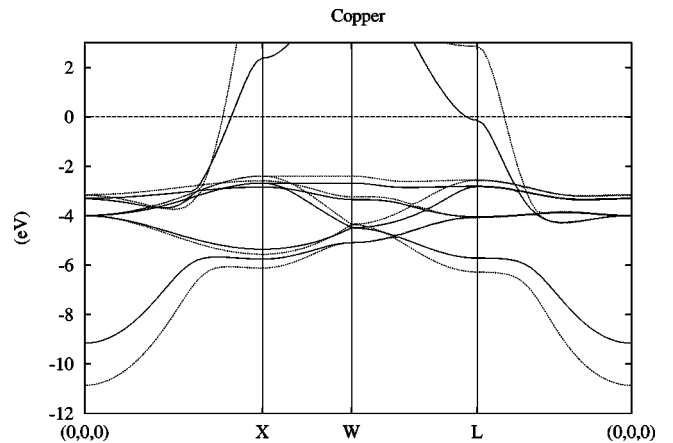
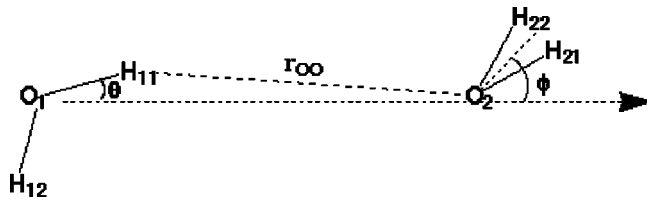


FIG. 5. Copper band structure obtained for two different basis sets: (i) sp^3d^5 (solid lines) and (ii) sd^5 (dotted lines). The dashed line represents the Fermi energy for the sp^3d^5 calculation. In this figure, the Fermi energy for the sd^5 calculation (not shown) lies at 1.36 eV.

FIG. 6. H₂O dimer.

ball” orbitals with a cutoff radius of $r_c = 4.5\alpha_B$; (ii) (solid lines) an sp^3d^5 basis set obtained from the previous one adding p orbitals with a cutoff radius of $r_c = 4.5\alpha_B$. Both the atomic and solid calculations have been performed using the LDA for the exchange-correlation interactions. In a similar approach as in the GaN results, we have corrected the two-center exchange-correlation matrix elements. The sd^5 basis orbitals are calculated by solving the the atomic problem with occupation numbers $n_s^0 = 1$ and $n_d^0 = 10$ instead of the atomic values $n_s^0 = 2$ and $n_d^0 = 9$, because the self-consistent occupations numbers in the solid are going to be closer to the first set of values.

In order to facilitate the comparison between the two calculations, the sd^5 band structure has been shifted upwards so that the lowest d bands coincide at the Γ point with the d bands of the sp^3d^5 band structure. The overall agreement of these band structures with more sophisticated calculations (which can be found in Ref. 65) is quite good. For the sd^5 band structure, the d bands are quite well described, while the sp band is only roughly represented due to the absence of the p orbitals in the basis set. The addition of p orbitals in the basis set has a minor effect on the d bands, but, as expected, improves significantly the description of the parabolic sp band. For Cu, we calculate the lattice parameter to be $a = 3.57 \text{ \AA}$ and the bulk modulus to be $B = 1.61 \text{ Mbars}$, compared with the experimental results of $a = 3.6 \text{ \AA}$ and $B = 1.34 \text{ Mbars}$, respectively.

C. H₂O dimer

Hydrogen bonding has significant relevance in biological systems. The inability of the SN method to accurately por-

tray hydrogen-bonded systems is inherently due to the lack of GGA exchange-correlation functionals within the method. Availability of the BLYP exchange-correlation functional in the improved method allows performing simulations where hydrogen bonding is considered. As a model test case for demonstrating the performance of FIREBALL to such systems, results of the H₂O dimer (see Fig. 6) are presented in Table II. For the results presented here, we use a double-numerical basis set with the following cutoffs: H, $r_c = 4.1$ and O, $r_c = 3.8, 4.1$. These cutoffs are slightly longer than what would be obtained using the cutoffs suggested in Sec. II A. These longer cutoffs are required for properly obtaining the hydrogen-bonding characteristics, which is a longer-range interaction compared with covalent bonds found in crystals.

The structural results are quite comparable with the results of others, but the binding energy is high. Results from a similar DFT local-orbital method (SIESTA) demonstrate that including an additional polarization basis set decreases the binding energy as compared with the strictly double-numerical basis set. Investigation of different and more extensive basis sets will be the topic of future work.

D. HMX structure and energetics

Additionally, FIREBALL was used to study a single gas-phase α -HMX molecule as a benchmark test case of organic molecules. HMX is important in many industrial and military applications because of its high detonation velocity. In the gas phase two nearly energetically equivalent polymorphs of HMX exist—a boat conformer and a chair conformer of the molecule as shown in Fig. 7. A minimal sp^3 basis set and the BLYP exchange-correlation functional predict that the energy difference between the two conformers is 190 kcal/mol. This significant overestimation affirms that the minimal basis set is insufficient for correctly predicting the energetics of many molecules, even though the “fireball” radii were picked to properly preserve trends in ionization energies.

TABLE II. Results of bondlengths, bondangles, and binding energy for the H₂O dimer. A comparison with the results from other methods are included—SIESTA (Perdew, Burke, and Ernzerhof exchange-correlation) with DN and DNP (Ref. 11), deMon with Perdew and Wang exchange/Perdew correlation (LCAO/PW) and Becke exchange/Perdew correlation (LCAO/BP) (Ref. 66), second-order Moller-Plesset calculations (MP2) (Ref. 67), and plane waves PLW (Ref. 68). A summary of the experimental results found in Ref. 66 are also included. The parameters are defined according to Fig. 6; lengths are in \AA angles are in degrees and the binding energies are in kcal/mol.

	This work	DN	DNP	LCAO/BP	LCAO/PW	MP2	PLW	Expt.
$r(\text{O}_1\text{-O}_2)$	2.98	2.752	2.902	2.886	2.887	2.911	2.70(2.98)	2.98 ± 0.01
$r(\text{O}_2\text{-H})$	1.01	0.996	0.981	0.979	0.981	0.957	0.961	
$\angle \text{HO}_2\text{H}$	104.6	111.2	106.2	106.2	104.4		106.2	
$r(\text{O}_1\text{-H}_{11})$	1.03	1.015	0.988	0.990	0.990	0.964	1.002	
$r(\text{O}_1\text{-H}_{12})$	1.02	0.997	0.980	0.977	0.979		0.981	
$\angle \text{HO}_1\text{H}$	100.8	110.8	104.7	106.2	106.0		107.3	
θ	-4.4	-2.6	-4.7	-7.0	-15.1	-4.5	-4.84	-6 ± 20
ϕ	58.4						59.4	57 ± 10
Binding En.	8.88	11.76	7.36	4.51	5.993	5.44	9.06(4.90)	5.44 ± 0.7

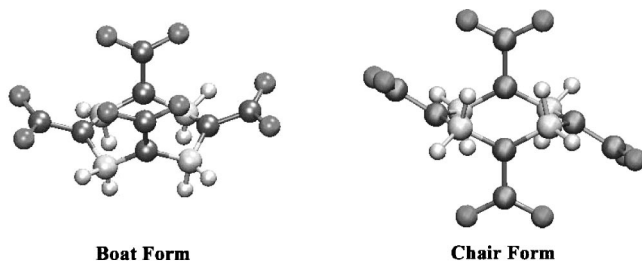


FIG. 7. The boat and chair gas-phase conformers of HMX.

Because of the need to maintain proper energetic trends in the orbitals, different cutoffs are generally needed for s and p shells. This is an improvement over the original SN method that forced all shells on a given atom to have the same cutoff. Specifically, for the s and p shells, respectively, we choose $H(r_c=3.8)$, $C(r_c=4.1,4.4)$, $N(r_c=3.7,4.1)$, and $O(r_c=3.5,3.8)$ for the HMX results presented here. DN basis sets were generated by calculating the lowest-lying excited atomic states, subject to the same r_c boundary conditions and orthonormality constraints. Improving the basis set to DN ($ss^*p^3p^{*3}$) reduces the energy difference between the chair and boat conformers to 6.8 kcal/mol. This energy difference gives the same thermodynamic trend as the experimental results (the boat conformer is energetically higher) and demonstrates the need for an adequate basis set to get the quantitative nature of the difference correct. It is important to note that both basis sets predict the correct energetic trend.

For comparison, results found using several different levels of theory are presented. Using single- z basis set BLYP/STO-3G with GAUSSIAN 98 (Ref. 69) (closest equivalence to our single-numerical basis set) predicts the energy difference to be 1.4 kcal/mol in the wrong direction. BLYP/6-31G (closest equivalence to our double-numerical basis set) predicted that the boat form is 1.4 kcal/mol higher in energy than the chair form. Increasing the basis set size to 6-311G** reduces this energy difference to 0.81 kcal/mol. Mixing in exact exchange with B3LYP/6-311G** increased this energy difference to 2.33 kcal/mol. Chakraborty *et al.* reported results of 3.5 kcal/mol for B3LYP/6-311G**/MP2/6-311G** and 2.5 kcal/mol for B3LYP/6-31G*.⁷⁰ Clearly none of these results have converged to the chemically “exact” answer. Based upon these wide range of results, our BLYP/DN results are reasonable.

Improving the level of basis set and theory should improve upon our BLYP/DN results, although it is worth noting that the energy differences do not always converge uniformly, even if the separate energies are converging uniformly. Convergence with respect to basis-set size is known to be erratic for correlated methods such as MP2.⁷¹ Improvements in theory, such as going from Hartree-Fock to MP2, can cause pathological results.⁷² A greater dependence on basis set size should be expected in B3LYP, rather than BLYP because of the exact exchange contribution. Because of these issues, the level of theory and basis set must be properly chosen and well balanced for all species studied. We find that the BLYP/DN method in FIREBALL obtains such a balance, although B3LYP would most likely necessitate extending the basis further to B3LYP/DNP. Adding improve-

ments such as polarization basis functions, exact exchange will significantly increase the memory and CPU requirements during the computation, thus the need for a linear-scaling algorithm is even greater for larger systems as these demands are increased. Work on this extension is currently underway, along with a systematic study of DN and DNP basis-set design.

IV. CONCLUDING REMARKS

Improvements to the Sankey-Niklewski *ab initio* tight-binding method have been presented. The main feature of this new method, called FIREBALL, is that the flexibility of the basis set is incorporated through implementation of double-numerical basis set capabilities as well as implementation of d orbitals. Other major improvements to the method include the following. First, the pseudopotential is now of the generalized norm-conserving separable form of the Hamann type or the Troullier-Martins type, thus simplifying the representation of the nonlocal pseudopotential Hamiltonian matrix elements into a separable form.^{2,23,33,34} Second, the representation of the exchange-correlation interactions have been simplified and more accurately portrayed according to the Horafeld-multicenter-expansion approximation (up to three-center terms).¹² Third, the self-consistent method of Demkov *et al.*¹³ has been implemented to allow charge transfer between atomic constituents, which is important when calculating systems with significant differences in the electronegativity of those constituents. The combination of these three main implementations as well as other minor improvements to the method have produced a method that has wider applications to the type of systems that can be calculated.

The effectiveness and versatility of FIREBALL has been demonstrated by applying the method to several systems—Cu, GaN, the H₂O dimer system, and a gas-phase HMX molecule. In the cases of Cu and GaN the band structures are presented. In all cases, addition of d orbitals, a feature not contained in the Sankey-Niklewski method, yields qualitatively better features of the band structure and quantitatively better band-gap energies for GaN. The Cu band structure was not obtainable with the Sankey-Niklewski method because of the lack of d orbitals, and with this new flexibility, we obtain an accurate representation of the Cu band structure. Finally, to demonstrate the flexibility of the method, results for the H₂O dimer and HMX were presented.

ACKNOWLEDGMENTS

The authors would like to thank the following people for useful discussions regarding this ongoing project. G. Adams, A. Chizmeshya, D. Drabold, R. Evans, S. Iyengar, K. Schmidt, T. Sewell, J. Tomfohr, J. Wang, and W. Windl. K.R.G. would like to acknowledge the NSF for a CISE post-doctoral fellowship. This research is in part funded by The University of Utah Center for the Simulation of Accidental Fires and Explosions (C-SAFE), the Department of Energy,

Lawrence Livermore National Laboratory, under Subcontract No. B341493, the Deutsche Forschungsgemeinschaft under Contract Nos. FR 1426/2-1 and GRK 176/3-99, the CICyT (Spain) under Contract No. PB-97-0028, and Motorola, Inc.

(Semiconductor Products Sector). In addition, an allocation of computer time from the Center for High Performance Computing at the University of Utah is gratefully acknowledged.

- ¹O. F. Sankey and D. J. Nikleswki, Phys. Rev. B **40**, 3979 (1989).
- ²D. R. Hamann, M. Schlüter, and C. Chiang, Phys. Rev. Lett. **43**, 1494 (1979).
- ³G. B. Bachelet, D. R. Hamann, and M. Schlüter, Phys. Rev. B **26**, 4199 (1982).
- ⁴J. Harris, Phys. Rev. B **31**, 1770 (1985).
- ⁵W. M. C. Foulkes and R. Haydock, Phys. Rev. B **39**, 12 520 (1989).
- ⁶O. F. Sankey, A. A. Demkov, W. Windl, J. H. Fritsch, J. P. Lewis, and M. Fuentes-Cabrera, Int. J. Quantum Chem. **69**, 327 (1998).
- ⁷G. B. Adams, O. F. Sankey, M. O'Keefe, J. B. Page, and D. A. Drabold, Science **256**, 1792 (1992).
- ⁸A. Caro, D. A. Drabold, and O. F. Sankey, Phys. Rev. B **49**, 6647 (1994).
- ⁹M. Cobb, D. A. Drabold, and R. L. Cappelletti, Phys. Rev. B **54**, 12 162 (1996).
- ¹⁰S. H. Yang, D. A. Drabold, J. B. Adams, P. Ordejón, and K. Glassford, J. Phys.: Condens. Matter **9**, L39 (1997).
- ¹¹D. Sánchez-Portal, P. Ordejón, E. Artacho, and J. M. Soler, Int. J. Quantum Chem. **65**, 453 (1997).
- ¹²A. Horsfield, Phys. Rev. B **56**, 6594 (1997).
- ¹³A. A. Demkov, J. Ortega, O. F. Sankey, and M. P. Grumbach, Phys. Rev. B **52**, 1618 (1995).
- ¹⁴J. P. Lewis, T. D. Sewell, R. B. Evans, and G. A. Voth, J. Chem. Phys. B **104**, 1009 (2000).
- ¹⁵J. Ortega, A. L. Yeyati, and F. Flores, Appl. Surf. Sci. **123**, 131 (1998).
- ¹⁶J. Ortega, F. Flores, and A. L. Yegati, Phys. Rev. B **58**, 4548 (1998).
- ¹⁷J. Avila, A. Mascaraque, E. G. Michel, M. C. Asensio, G. LeLay, J. Ortega, R. Pérez, and F. Flores, Phys. Rev. Lett. **82**, 442 (1999).
- ¹⁸J. Ortega, R. Pérez, and F. Flores, J. Phys.: Condens. Matter **12**, L21 (2000).
- ¹⁹A. A. Demkov and O. F. Sankey, Phys. Rev. Lett. **83**, 2083 (1999).
- ²⁰F. J. García-Vidal, J. Merino, R. Pérez, R. Rincón, J. Ortega, and F. Flores, Phys. Rev. B **50**, 10 537 (1994).
- ²¹J. Ortega, J. P. Lewis, and O. F. Sankey, Phys. Rev. B **50**, 10 516 (1994).
- ²²J. P. Lewis, P. Ordejón, and O. F. Sankey, Phys. Rev. B **55**, 6880 (1997).
- ²³D. R. Hamann, Phys. Rev. B **40**, 2980 (1989).
- ²⁴M. Finnis, J. Phys.: Condens. Matter **2**, 331 (1990).
- ²⁵J. P. Perdew and A. Zunger, Phys. Rev. B **23**, 5048 (1981).
- ²⁶J. P. Perdew, Phys. Rev. B **33**, 7406 (1986).
- ²⁷C. Lee, W. Yang, and R. G. Parr, Phys. Rev. B **37**, 785 (1988).
- ²⁸A. D. Becke, Phys. Rev. A **38**, 3098 (1988).
- ²⁹J. P. Perdew, K. A. Jackson, M. R. Pederson, D. J. Singh, and C. Fiolhais, Phys. Rev. B **46**, 6671 (1992).
- ³⁰J. P. Perdew and Y. Wang, Phys. Rev. B **45**, 13 244 (1992).
- ³¹J. P. Perdew, K. Burke, and M. Ernzerhof, Phys. Rev. Lett. **77**, 3865 (1996).
- ³²J. P. Perdew, K. Burke, and Y. Wang, Phys. Rev. B **54**, 16 533 (1996).
- ³³N. Trouiller and J. L. Martins, Phys. Rev. B **43**, 1993 (1991).
- ³⁴M. Fuchs and M. Scheffler, Comput. Phys. Commun. **119**, 67 (1999).
- ³⁵L. Kleinman and D. M. Bylander, Phys. Rev. Lett. **48**, 1425 (1982).
- ³⁶X. Gonze, R. Stumpf, and M. Scheffler, Phys. Rev. B **44**, 8503 (1991).
- ³⁷D. M. Ceperley and G. J. Alder, Phys. Rev. Lett. **45**, 566 (1980).
- ³⁸A. E. DePristo and J. D. Kress, J. Chem. Phys. **86**, 1425 (1987).
- ³⁹R. Colle and D. Salvetti, Theor. Chim. Acta **37**, 329 (1975).
- ⁴⁰B. G. Johnson, P. M. W. Gill, and J. A. Pople, J. Chem. Phys. **98**, 5612 (1993).
- ⁴¹H. M. Polatoglou and M. Methfessel, Phys. Rev. B **37**, 10 403 (1988).
- ⁴²A. Read and R. Needs, J. Phys.: Condens. Matter **1**, 7565 (1989).
- ⁴³E. Zaremba, J. Phys.: Condens. Matter **2**, 2479 (1990).
- ⁴⁴H. M. Polatoglou and M. Methfessel, Phys. Rev. B **41**, 5898 (1990).
- ⁴⁵I. Robertson and B. Farid, Phys. Rev. Lett. **66**, 3265 (1991).
- ⁴⁶B. Farid, V. Heine, G. E. Engel, and I. Robertson, Phys. Rev. B **48**, 11 602 (1993).
- ⁴⁷J. Almlöf, in *Modern Electronic Structure Theory, Part I*, edited by D. R. Yarkony (World Scientific, New Jersey, 1995), p. 110.
- ⁴⁸J. P. Lewis, K. R. Glaesemann, S. D. Shellman, K. Sikorski, and G. A. Voth, J. Comput. Phys. (2001).
- ⁴⁹M. W. Schmidt, K. K. Baldrige, J. A. Boatz, S. T. Elbert, M. S. Gordon, J. H. Jensen, S. Koseki, N. Matsunaga, K. A. Nguyen, S. Su, T. L. Windus, M. Dupois, and J. J. A. Montgomery, J. Comput. Chem. **14**, 1347 (1993).
- ⁵⁰B. Delley, J. Chem. Phys. **92**, 508 (1990).
- ⁵¹S. Nakamura, M. Senoh, and T. Mukai, Jpn. J. Appl. Phys., Part 2 **30**, L1708 (1991).
- ⁵²S. Nakamura, M. Senoh, S. Nagahama, N. Iwasa, T. Yamada, T. Matashushita, H. Kiyoku, and Y. Sugimoto, Jpn. J. Appl. Phys., Part 2 **35**, L74 (1996).
- ⁵³Morkoç, S. Strite, G. B. Gao, M. E. Lin, B. Sverdlov, and M. Burns, J. Appl. Phys. **76**, 1363 (1994).
- ⁵⁴S. Strite and H. Morkoç, J. Vac. Sci. Technol. B **10**, 1237 (1992).
- ⁵⁵V. Fiorentini, M. Methfessel, and M. Scheffler, Phys. Rev. B **47**, 13 353 (1993).
- ⁵⁶J. Neugebauer and C. V. de Walle, Phys. Rev. B **50**, 8067 (1994).
- ⁵⁷C. Stampfl and C. V. de Walle, Phys. Rev. B **59**, 5521 (1999).
- ⁵⁸W. M. C. Foulkes, Ph.D. thesis, University of Cambridge, 1985.
- ⁵⁹T. Lei, M. Fanciulli, R. J. Molnar, T. D. Moustakas, R. J. Graham, and J. Scanlon, Appl. Phys. Lett. **59**, 944 (1991).
- ⁶⁰M. E. Sherwin and T. J. Drummond, J. Appl. Phys. **69**, 8423 (1991).

- ⁶¹S. Strite, J. Ruan, Z. Li, N. Manning, A. Salvador, H. Chen, D. J. Smith, W. J. Choyke, and H. Morkoç, *J. Vac. Sci. Technol. B* **9**, 1924 (1991).
- ⁶²B. Paulos, F.-H. Shi, and H. Stoll, *J. Phys.: Condens. Matter* **9**, 2745 (1997).
- ⁶³S. A. Ding, G. Neuhold, J. H. Weaver, P. Häberle, K. Horn, O. Brandt, H. Yank, and K. Ploog, *J. Vac. Sci. Technol. A* **14**, 819 (1996).
- ⁶⁴D. Vogel, P. Krüger, and J. Pollman, *Phys. Rev. B* **55**, 12 836 (1996).
- ⁶⁵D. A. Papaconstantopoulos, *Handbook of the Band Structure of Elemental Solids* (Plenum, New York, 1998).
- ⁶⁶F. Sim, A. St-Amant, I. Papai, and D. Salahub, *J. Am. Chem. Soc.* **114**, 4391 (1992).
- ⁶⁷M. Frisch, J. D. Bene, J. Binkley, and H. S. III, *J. Chem. Phys.* **84**, 2279 (1986).
- ⁶⁸R. Barnett and U. Landman, *Phys. Rev. B* **48**, 2081 (1993).
- ⁶⁹M. J. Frisch, G. W. Trucks, H. B. Schlegel, E. Scuseria, M. A. Robb, J. R. Cheeseman, V. G. Zakrzewski, J. A. Montgomery, Jr., R. E. Stratmann, J. C. Burant, S. Dapprich, J. M. Millam, A. D. Daniels, K. N. Kudin, M. C. Strain, O. Farkas, J. Tomasi, V. Barone, M. Cossi, R. Cammi, B. Mennucci, C. Pomelli, C. Adamo, S. Clifford, J. Ochterski, G. A. Petersson, P. Y. Ayala, Q. Cui, K. Morokuma, D. K. Malick, A. D. Rabuck, K. Raghavachari, J. B. Foresman, J. Cioslowski, J. V. Ortiz, B. B. Stefanov, G. Liu, A. Liashenko, P. Piskorz, I. Komaromi, R. Gomperts, R. L. Martin, D. J. Fox, T. Keith, M. A. Al-Laham, C. Y. Peng, A. Nanayakkara, C. Gonzalez, M. Challacombe, P. M. W. Gill, B. Johnson, W. Chen, M. W. Wong, J. L. Andres, C. Gonzalez, M. Head-Gordon, E. S. Replogle, J. A. Pople, *GAUSSIAN 98, Revision A.6* (Gaussian, Inc., Pittsburgh, PA, 1998).
- ⁷⁰D. Chakraborty, R. P. Muller, S. Dasgupta, and I. W. A. Goddard, *J. Phys. Chem. A* (2000).
- ⁷¹A. K. Wilson, D. E. Woon, K. A. Peterson, and J. T. H. Dunning, *J. Chem. Phys.* **110**, 7667 (1999).
- ⁷²M. S. Gordon, M. W. Schmidt, G. M. Chaban, K. R. Glaesemann, W. J. Stevens, and C. Gonzalez, *J. Chem. Phys.* **110**, 4199 (1999).